

Origin of the 150-K Anomaly in LaFeAsO: Competing Antiferromagnetic Interactions, Frustration, and a Structural Phase Transition

T. Yildirim*

*NIST Center for Neutron Research, National Institute of Standards and Technology, Gaithersburg, Maryland 20899, USA
and Department of Materials Science and Engineering, University of Pennsylvania, Philadelphia, Pennsylvania 19104, USA*

(Received 17 April 2008; published 1 August 2008)

From all-electron fixed-spin-moment calculations we show that ferromagnetic and checkerboard antiferromagnetic ordering in LaFeAsO are not stable and the stripe antiferromagnetic configuration with $M(\text{Fe}) = 0.48\mu_B$ is the only stable ground state. The main exchange interactions between Fe ions are large, antiferromagnetic, and frustrated. The magnetic stripe phase breaks the tetragonal symmetry, removes the frustration, and causes a structural distortion. These results successfully explain the magnetic and structural phase transitions in LaFeAsO recently observed by neutron scattering. The presence of competing strong antiferromagnetic exchange interactions suggests that magnetism and superconductivity in doped LaFeAsO may be strongly coupled, much like in the high- T_c cuprates.

DOI: [10.1103/PhysRevLett.101.057010](https://doi.org/10.1103/PhysRevLett.101.057010)

PACS numbers: 74.25.Jb, 67.30.hj, 74.25.Kc, 75.30.Fv

The recent discovery of superconductivity at T_c 's up to 50 K in layered rare-earth (R) transition metal (T) pnictide(Pn)-oxide quaternary compounds $ROTPn$ ($R = \text{La, Ce, Sm}$, $T = \text{Mn, Fe, Co, Ni}$, $\text{Pn} = \text{P, As}$) [1–4] has sparked enormous interest in this class of materials. These are the first noncopper based materials that exhibit superconductivity at relatively high temperatures upon electron (O_{1-x}F_x) [1–4] and hole doping ($\text{La}_{1-x}\text{Sr}_x$) [5] of their nonsuperconducting parent compounds, just like high- T_c cuprates. Clearly, the understanding of electronic, magnetic, and structural properties of the parent compound LaFeAsO is the key to determining the underlying mechanism that makes these materials superconduct upon electron or hole doping.

The early theoretical studies identified several candidate ground states for LaFeAsO such as a nonmagnetic metal near a ferromagnetic or antiferromagnetic (AFM) instability [6–8] and a simple antiferromagnetic semimetal [9,10]. The most recent calculations suggested that LaFeAsO has an antiferromagnetic spin-density-wave (SDW) instability due to Fermi-surface nesting [11,12]. Experimental studies including resistivity and magnetic susceptibility show a small but very clear anomaly near 150 K in LaFeAsO [1,11]. The origin of this anomaly has been very recently determined by neutron scattering studies [13]. It has been found that LaFeAsO indeed exhibits the predicted SDW-like antiferromagnetic long-range ordering with a small $0.35\mu_B$ per Fe moment followed by a small structural distortion [13]. However, there is no proposed microscopic theory that explains the origin of the observed structural distortion. It is also not clear if the magnetic and structural phase transitions are related to each other. Finally, given the fact that both the cuprates and LaFeAsO exhibit antiferromagnetic ordering, one wonders how strong and what kind of magnetic spin fluctuations are present in the 2D Fe-square lattice of LaFeAsO.

In this Letter, from accurate all-electron density functional calculations we try to answer some of these questions. We find that the effective nearest-neighbor (NN) and next-nearest-neighbor (NNN) magnetic interactions between Fe ions in the square lattice are large, comparable to each other, and more importantly they are antiferromagnetic. This forces the Fe spins along the square diagonal to order antiparallel, resulting in two interpenetrating square AFM sublattices. Since in this configuration we have one parallel and one antiparallel alignment of the spins along the square axes, the nearest-neighbor exchange interaction is totally frustrated. The system lowers its energy further by a structural distortion that makes the two sides of the square lattice inequivalent. These results including the magnetic moment of the Fe ions and the degree of structural distortion are in excellent agreement with the recent neutron data [13]. Therefore, we have a nice working microscopic theory that explains the details of both the magnetic and structural properties of the undoped parent compound LaFeAsO. Our theory also brings attention to the presence of the strong competing antiferromagnetic interactions in this class of materials. Even though electron doping seems to destroy the long-range magnetic order, the short-range spin fluctuations will always be present and probably play an important role in the superconducting phase, much like the high- T_c cuprates.

The calculations were done using the full-potential linearized augmented plane wave (FP-LAPW) method, within local density approximation using Perdew-Wang–Ceperlye–Alder exchange correlation [14,15]. We also used the ultrasoft pseudopotential plane wave method [16] for cross-checking of our results and for phonon calculations. We considered $\sqrt{2} \times \sqrt{2}$ supercell of the primitive cell of LaFeAsO which is shown in Fig. 1. In order to determine the true ground state, we have considered four different cases. These are nonmagnetic (NM, i.e.,

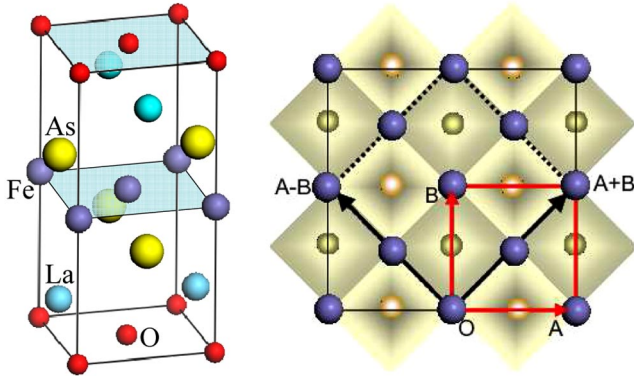


FIG. 1 (color online). (a) The crystal structure of LaFeAsO in space group $P4/nmmm$ with origin choice 1. (b) Top view of the FeAs plane and the relations between primitive and $\sqrt{2} \times \sqrt{2}$ supercell used in our calculations. The dark and light shaded areas indicate the As atoms below and above the Fe square lattice, respectively.

no spin polarization), ferromagnetic (FM), and the two different antiferromagnetic spin configurations shown in Fig. 2. The first one of the antiferromagnetic configurations is AFM1 where the nearest-neighbor spins are antiparallel to each other. The second antiferromagnetic configuration, AFM2, is shown in Fig. 2(b). In AFM2 the Fe spins along the square diagonal are aligned antiferromagnetically. This is the stripe phase which was first predicted from Fermi-surface nesting [11,12]. The AFM2 spin configuration can be considered as two interpenetrating simple square AFM sublattices [red and blue sublattices in Fig. 2(b)]. We note that since each Fe ion is at the middle of a square AFM lattice, the mean field at each spin site is zero. Hence one sublattice can be rotated freely with respect to the other sublattice without costing any energy. For this reason the AFM2 spin configuration is fully frustrated. In frustrated magnetic systems, it is known that the frustration is almost always removed by either a structural distortion or by thermal and quantum fluctuations [17,18]. From the clas-

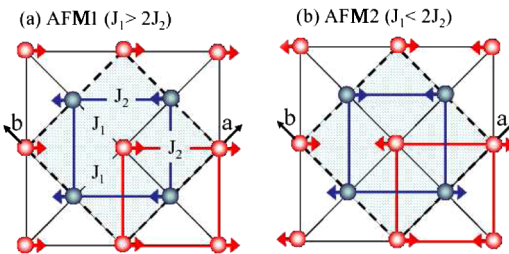


FIG. 2 (color online). Two antiferromagnetic configurations considered in this study. Left-hand panel shows the AFM1 configuration where nearest-neighbor spins are always aligned antiparallel. Right-hand panel shows the AFM2 configuration where the next-nearest-neighbor spins (i.e., J_2) are always aligned antiparallel. Note that this is the same stripe phase predicted from Fermi-surface nesting [11,12].

sical energies of AFM1 and AFM2, one sees that the AFM2 spin configuration is stabilized when $J_2 > J_1/2$.

In order to determine which spin configurations among NM, FM, AFM1, and AFM2 is the ground state, we have carried out FP-LAWP total energy calculations for each case. Since in spin-polarized calculations it is very easy to get a local minimum, we followed a different strategy. In our calculations we fixed the magnetic moment per Fe ion and then scanned the total energy as a function of Fe-magnetic moment. Our results are summarized in Fig. 3. The zero of energy is taken as the $M = 0$ case (i.e., NM calculation). From Fig. 3, it is clear that LaFeAsO has only one magnetic ground state which is AFM2. The ferromagnetic spin configuration always results in the highest energy regardless of the Fe magnetic moment. Similarly AFM1 ordering always yields energies higher than the NM case. For the AFM2 ordering, we see that the energy minimum occurs near the fixed moment calculation with $M = 1$. Repeating calculations where magnetization is not fixed, we obtained the optimum magnetic moment as $M = 0.87\mu_B$ per Fe. As we discuss below in detail, the Fe magnetic moment is further reduced almost by half when the structure is allowed to distort due to AFM2 stripe ordering.

In order to gain a better insight into the nature of the magnetic interactions present in the Fe square lattice of the LaFeAsO system, we map the calculated total energies of the FM, AFM1, and AFM2 configurations shown in Fig. 3(a) to a simple Heisenberg-like model $H = \sum_{i,j} J_{i,j} M_i M_j$ for a given fixed Fe moment M_i . For fully localized spin systems this is a perfect thing to do, but for the case of LaFeAsO this is only an approximation. Nevertheless, the calculated J 's should be a good indication of the magnetic interactions present in the system. We also note that these interactions are valid at temperatures close to magnetic ordering where the spin flippings are the relevant magnetic excitations (and not the spin waves) [19]. Figure 3(b) shows the *effective* J_1 and J_2 obtained from the energies of the FM, AFM1, and AFM2 at given

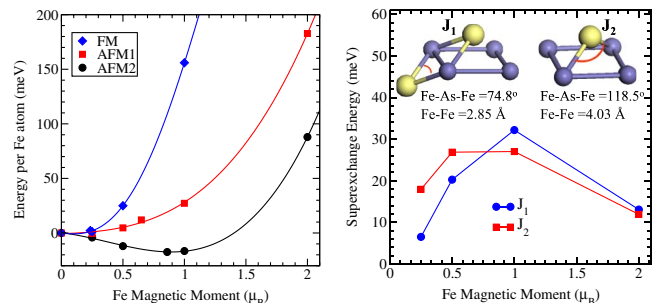


FIG. 3 (color online). (a) The total energy per Fe atom versus magnetic moment for FM, AFM1, and AFM2 spin configuration, indicating AFM2 is the only ground state of the system. (b) The magnetic interactions for NN and NNN Fe ions obtained from the energies of FM, AFM, and AFM2 configurations.

magnetic moment. The dependence of the J 's on the magnetic moment further suggests that the simple Heisenberg Hamiltonian is not a good model for this system. The calculations of magnetic interactions up to 3rd-nearest neighbor are in progress and will be discussed elsewhere [19]. Our initial results indicate that long-range interactions are small and J_1 (which is different for parallel and perpendicular to the stripe direction) and J_2 are the dominant interactions in the system [19]. From Fig. 3, it is clear that both J_1 and J_2 are quite large and positive (i.e., antiferromagnetic). J_2 is always larger than $J_1/2$ and therefore AFM2 structure is the only ground state for any given moment of the Fe ion. By looking at the exchange paths for J_1 and J_2 (shown in insets of Fig. 3), we notice that the Fe-As-Fe angle is around 75° and 120° for NN and NNN Fe pairs, respectively. Hence it makes sense that the 2nd NN exchange interaction is as strong as the NN exchange because the angle is closer to the optimum value of 180° . It is quite surprising and also very interesting that there are strong and competing antiferromagnetic interactions in the LaFeAsO system that result in a totally frustrated AFM2 spin configuration.

We next discuss the implication of the magnetically frustrated AFM2 configuration on the structural distortion recently observed by neutron scattering [13]. In order to demonstrate the structural distortion by AFM2 stripe ordering, we calculated the total energy of the AFM2 spin configuration as a function of the γ angle as shown in the inset of Fig. 4. When $\gamma = 90^\circ$, we have the original

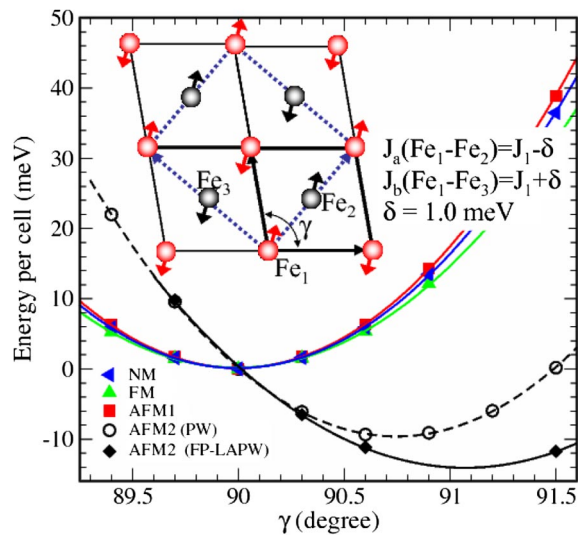


FIG. 4 (color online). The total energy per cell versus the angle γ for nonmagnetic (NM), ferromagnetic (FM), and two antiferromagnetic (AFM1 and AFM2) spin configurations. Note that only the AFM2 spin configuration yields structural distortion. The inset shows that as γ increases, the ferromagnetically aligned Fe ions (i.e., $\text{Fe}_1\text{-Fe}_2$) get closer while the antiferromagnetically aligned ions (i.e., $\text{Fe}_1\text{-Fe}_3$) move apart, breaking the fourfold symmetry and thus the degeneracy of the d_{xz} and d_{yz} orbitals.

tetragonal cell. Once the γ deviates from 90° , the original $\sqrt{2} \times \sqrt{2}$ structure (shown as a dashed line) is no longer tetragonal but orthorhombic (i.e., the cell length along the a and b axes are no longer equal). The total energy versus γ plot shown in Fig. 4 clearly indicates that the structure is indeed distorted with $\gamma = 91.0^\circ$, which is in good agreement with the experimental value of 90.3° . We note that plane wave calculations (dotted line) are in excellent agreement with the FP-LAPW method except that the magnetization of the Fe ion comes out very large. From the FP-LAPW method we get $M = 0.48\mu_B$, which is in excellent agreement with the experimental value of $0.35\mu_B$. The net energy gain by the structural distortion is about 12 meV per cell, which is of the same order as the temperature at which this phase transition occurs. We also considered two types of AFM2 where the spins along the short axis are aligned parallel or antiparallel. These two configurations are no longer equivalent. According to our calculations the configuration in which the spins are ordered parallel along the short axis is the ground state. We note that the neutron Bragg peaks $(1, 0, l)$ and $(0, 1, l)$ are zero and nonzero for these two spin-configurations and therefore it should be possible to determine the exact spin configuration from neutron powder diffraction.

In order to make sure that the structural distortion is driven mainly by AFM2 ordering and not by other effects, we have also calculated total energy versus γ angle for other spin configurations including the nonmagnetic case. We note that for $\gamma = 90^\circ$, the orbitals d_{xz} and d_{yz} are degenerate and therefore one may think that the system is subject to symmetry lowering for reasons similar to those in a Jahn-Teller distortion. However, as shown in Fig. 4, we do not see any distortion for any of the NM, FM, and AFM configurations. Therefore, the experimentally observed structural distortion is due to AFM2 stripe order-

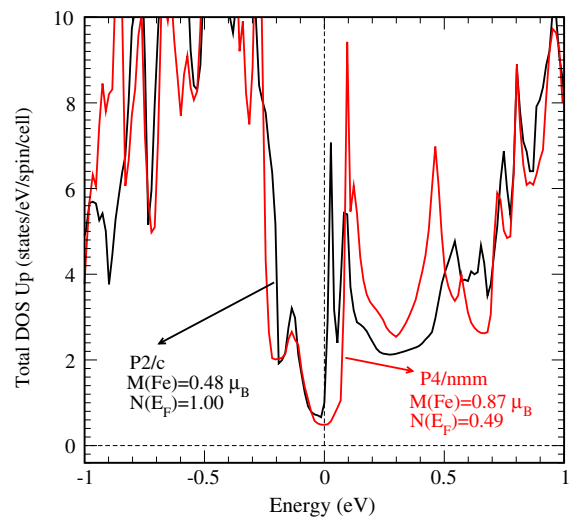


FIG. 5 (color online). The total electronic DOS of LaFeAsO for high ($P4/nmm$) and low ($Cmma$ or $P2/c$) symmetry phases.

TABLE I. The symmetries and energies (in meV) of the optical phonons of LaFeAsO in $P4/nmm$ and $Cmma$ phases. The energies of the IR-active modes are taken from Ref. [11]. The asterisk indicates a significant disagreement. The details of calculations and the animations of the modes can be found in Ref. [20]

$\Gamma(P4/nmm) = 2A_{1g}(R) + 4A_{2u}(IR) + 4E_u(IR) + 4E_g(R) + 2B_{1g}(R)$														
$\Gamma(Cmma) = 2A_g(R) + 2B_{1g}(R) + 4B_{1u}(IR) + 4B_{2g}(R) + 4B_{2u}(IR) + 4B_{3g}(R) + 4B_{3u}(IR)$														
$P4/nmm$	$Cmma$	IR	$P4/nmm$	$Cmma$	IR	$P4/nmm$	$Cmma$	IR	$P4/nmm$	$Cmma$	IR	$P4/nmm$	$Cmma$	IR
E_u 7.3	7.4–7.5	...	A_{2u} 9.9	10.1	12.1	E_g 14.0	14.1–14.2	...	E_g 17.6	17.7–17.8	...	A_{1g} 22.1	22.3	...
A_{1g} 24.9	25.1	...	B_{1g} 26.6	26.9	...	A_{2u} 31.2	31.6	30.9	E_u 33.7	34.0–34.1	33.2	B_{1g} 35.2	35.6	...
E_g 35.6	35.9–36.1	...	E_u 34.3	34.6–34.7	42.0*	A_{2u} 48.6	49.1	53.8	E_g 51.6	51.8–52.6	...			

ing, which results in different occupancy for the d_{xz} and d_{yz} orbitals and therefore breaks the tetragonal symmetry.

We now briefly discuss the effect of the structural distortion on the electronic structure and the zone center phonons. The details will be published elsewhere [19]. Figure 5 shows the electronic density of states before and after the structural distortion with the AFM2 ordering in $\sqrt{2} \times \sqrt{2}$ structure. The $N(E_F)$ in both phases are quite small compared to previous calculations in which incorrect AFM ordering was considered. It seems that AFM2 is stabilized further over AFM due to pseudogap formation in the iron d orbitals near E_F . It is apparent that the distortion has significant effect both on the $N(E_F)$ and the Fe magnetization. Interestingly, the $N(E_F)$ is doubled while the magnetization is reduced by half due to structural distortion. The increase in the $N(E_F)$ is consistent with the resistivity measurement which shows that LaFeAsO exhibits metallic behavior after the transition [11]. Finally, we note the existing several sharp van Hove-like kinks in the density of states (DOS). In particular, the distortion brings one of these kinks just next to the Fermi energy. Hence, with a small electron doping, it is quite possible to increase the $N(E_F)$ significantly. The effect of such electron doping is under study and will be reported elsewhere [19].

Finally we explain why Dong *et al.* did not see any evidence of the structural phase transition in their optical IR measurements [11]. From the symmetry decomposition of the optical phonons in both $P4/nmm$ and $Cmma$ phases (see Table I), we note that the distortion does not introduce any new IR-active modes but rather just splits the doubly degenerate modes into nondegenerate ones. However, the splitting is quite small; the largest is around 0.2 meV. This explains why no new modes appear in the optical measurements after the transition. We also note that the agreement for the energies of the zone center phonons with IR data is not as good as one expects. In particular, the E_u mode observed at 42 meV is calculated to be 35 meV, a significantly lower value. Interestingly, this particular mode has a strong temperature dependence [11]. We checked that the disagreement is not due to anharmonic phonons. The calculated phonons are harmonic, unlike those observed in the MgB₂ superconductor [21]. We hope that our observation will motivate others to look at the zone-center phonons carefully to understand the discrepancy.

In conclusion, we have presented a first-principles study of the exchange interactions between Fe ions and their effect on the magnetic and structural properties of the parent compound LaFeAsO of the newly discovered high temperature superconductor LaFeAsO_{1-x}F_x. The competing strong antiferromagnetic exchange interactions and the frustrated ground state suggest that LaFeAsO has many common magnetic properties with the undoped parent component of the high- T_c cuprates.

The author acknowledges useful discussions with C. Cruz, R. L. Cappelletti, Q. Huang, J. W. Lynn, I. I. Mazin, W. Ratcliff, and D. J. Singh.

*taner@nist.gov

- [1] Y. Kamihara, T. Watanabe, M. Hirano, and H. Hosono, *J. Am. Chem. Soc.* **130**, 3296 (2008).
- [2] X. H. Chen *et al.*, arXiv:0803.3603v2.
- [3] G. F. Chen *et al.*, arXiv:0803.3790v2.
- [4] Z. A. Ren, arXiv:0803.4283v1.
- [5] H. H. Wen, G. Mu, L. Fang, H. Yang, and X. Y. E. Zhu, *Europhys. Lett.* **82**, 17009 (2008).
- [6] D. J. Singh and M.-H. Du, *Phys. Rev. Lett.* **100**, 237003 (2008).
- [7] Gang Xu *et al.*, arXiv:0803.1282.
- [8] K. Haule, J. H. Shim, and G. Kotliar, arXiv:0803.3236.
- [9] C. Cao, P. J. Hirschfeld, and H. P. Cheng, arXiv:0803.3236.
- [10] F. J. Ma and Z. Y. Lu, arXiv:0803.3286.
- [11] J. Dong *et al.*, *Europhys. Lett.* **83**, 27006 (2008).
- [12] I. I. Mazin, D. J. Singh, M. D. Johannes, and M. H. Du, arXiv:0803.2740.
- [13] C. de la Cruz, Q. Huang, J. W. Lynn, J. Li, W. Ratcliff II, H. A. Mook, G. F. Chen, J. L. Luo, N. L. Wang, and Pengcheng Dai, *Nature (London)* **453**, 899 (2008).
- [14] P. Blaha, K. Schwarz, P. Sorantin, and S. B. Trickey, *Comput. Phys. Commun.* **59**, 399 (1990).
- [15] <http://exciting.sourceforge.net/>.
- [16] <http://www.pwscf.org>.
- [17] T. Yildirim, A. B. Harris, and E. F. Shender, *Phys. Rev. B* **53**, 6455 (1996).
- [18] S. H. Lee, C. Broholm, T. H. Kim, W. Ratcliff II, and S.-W. Cheong, *Phys. Rev. Lett.* **84**, 3718 (2000).
- [19] T. Yildirim, arXiv:0807.4351.
- [20] <http://www.ncnr.nist.gov/staff/taner/laofeas>.
- [21] T. Yildirim *et al.*, *Phys. Rev. Lett.* **87**, 037001 (2001).